Journal of Food Engineering 104 (2011) 123–133

Contents lists available at ScienceDirect

Journal of Food Engineering

journal homepage: www.elsevier.com/locate/jfoodeng

κ-Carrageenan–sodium caseinate microgel production by atomization: Critical analysis of the experimental procedure

F.A. Perrechil, A.C.K. Sato, R.L. Cunha *

Department of Food Engineering, University of Campinas (UNICAMP), Faculty of Food Engineering, 13083-862 Campinas, SP, Brazil

ARTICLE INFO

Article history:
Received 8 September 2010
Received in revised form 29 November 2010
Accepted 2 December 2010
Available online 9 December 2010

Keywords:
Extrusion
Ionic gelation
Microscopy
Rheology

ABSTRACT

The influence of atomization process to produce κ-carrageenan and κ-carrageenan/sodium caseinate microgels was studied experimentally (aspect ratio and particle size distribution) and theoretically (dimensionless parameters). Moreover, rheological behavior of microgel suspensions was evaluated to examine their potential application in food products. Experimental results demonstrated that the size of microgels was influenced by feed flow rate, compressed air flow rate and composition of solutions, while their shape depended on the viscosity and surface tension of biopolymer solutions. Regarding the dimensionless numbers, higher values of Reynolds number of liquid layer ($Re_{\lambda l}$) and Weber number (We_l) led to smaller particles, while the decrease of Ohnesorge number (Oh) was related to lower sphericity of microgels. Rheological behavior of suspensions depended on not only the morphology and size of microgels, but also their composition. Incompatibility between κ-carrageenan and sodium caseinate in mixed microgels led to suspensions with more complex rheological behavior at determined biopolymer concentrations.

1. Introduction

The development and preparation of microgels have attracted great interest in a number of areas, including the pharmaceutical, medical, cosmetics, agricultural and food industries. Specifically in the food industry, the microgels can be used for a variety of applications, for example as the encapsulation matrix to protect active compounds, or as a texture modifier (Ellis and Jacquier, 2009). Regarding the control of product texture/rheology, the microgels can be used for different applications depending on their characteristics, such as composition, size and shape. Thus the knowledge of the rheology of microgel suspensions is a way to control the properties of such materials (Adams et al., 2004).

Among the ingredients that can be used to produce microgels, the polysaccharides are particularly attractive, mainly due to their technological properties and because they are generally recognized as safe (GRAS) (Keppeler et al., 2009). κ-Carrageenan is a polysaccharide with a structure composed of repeating D-galactose and 3,6-anhydrogalactose (3,6 AG) units, both sulfated and non-sulfated, joined by alternating α-(1,3) and β-(1,4) glycosidic links (De Ruiter and Rudolph, 1997; Imeson, 2000). Among the interesting technological properties of this polysaccharide, its gelling capacity is of special interest. The gelling process of κ-carrageenan involves a conformational transition from the coil to the helix form (De Ruiter and Rudolph, 1997), which depends on the temperature, the ionic strength and the biopolymer concentration (Morris et al., 1980; Meunier et al., 2001). κ-Carrageenan can also interact with other ingredients, especially with milk proteins (Imeson, 2000). Even though it has long been known that κ-carrageenan can form complexes with casein micelles (Dalgleish and Morris, 1988; Langendorff et al., 1997; Bourriot et al., 1999; Martin et al., 2006; Arltoft et al., 2007), few studies have evaluated the interaction between κ-carrageenan and sodium caseinate (Oakenfull et al., 1999; Belyakova et al., 2003; Ribeiro et al., 2004; Sabadini et al., in press).

Different methods have been established to produce microgels and most of them combine droplet/particle formation with the gelation process. Emulsion formation and extrusion mechanisms are some techniques in which droplet formation occurs prior to gelation (Burey et al., 2008). In the emulsion formation mechanism, the droplets are formed by dispersion of the biopolymeric solution into an oil phase, followed by the addition of a gelling agent to promote gelation (Poncelet et al., 1992; Reis et al., 2006; Ellis and Jacquier, 2009). In a different way, extrusion involves the formation of droplets by the use of a syringe or atomizer nozzle, and the droplets are then collected in a hardening solution containing the gelling agent, forming the microgels (Hunik and Tramper, 1993; Blandino et al., 1999). The gelation process commonly used to produce polysaccharide microgels via extrusion method is that of ionotropic gelation by diffusion setting (Zhang et al., 2007; Herrero et al., 2006; Smrdel et al., 2008), which involves the atomization of the polysaccharide solution into an ionic

* Corresponding author. Tel.: +55 19 35214047; fax: +55 19 35214027.
E-mail address: rosiane@fea.unicamp.br (R.L. Cunha).

0260-8774/
doi:10.1016/j.jfoodeng.2010.12.004

Nomenclature

$\bar{d}$	mean particle diameter obtained from equivalent sphere area ($\bar{d} = \sqrt{F_{max} \times F_{min}}$)
A_g	gas exit area
A_1	liquid exit area
AR	aspect ratio ($AR = F_{max}/F_{min}$)
b_g	thickness of the gas layer ($b_g = D_g - D_l$)
C	coefficient of proportionality that depends on the nozzle design (=1.2)
d_{32}	volume-surface mean diameter ($d_{32} = \sum n_i d_i^3 / \sum n_i d_i^2$)
D_g	gas nozzle exit diameter
D_1	diameter of the liquid jet
F_{max}	maximum Feret diameter
F_{min}	minimum Feret diameter
$\bar{d}_g$	geometric mean ($\bar{d}_g = \sum n_i \bar{d}_i / N$)
H	height from the atomizer nozzle to the KCl solution
N	total number of particles
n_i	number of particles with a determined diameter
Oh	Ohnesorge number ($Oh = \eta_1/\sqrt{\rho_1 \sigma D_1}$)
Re_g	Reynolds number of the gas ($Re_g = v_g b_g / \nu_g$)
$Re_{\lambda 1}$	Reynolds number of liquid layer ($Re_{\lambda_1} = (v_c - v_1)\lambda_1/\nu_1$)
SD	standard deviation of the geometric mean ($SD = \sqrt{\sum n_i(\bar{d}_i - \bar{d}_g)^2/N}$)
v	velocity (m/s)
v_c	velocity of the waves produced in the exit of nozzle $\left(v_c = \frac{\sqrt{\rho_1}v_1 + \sqrt{\rho_g}v_g}{\sqrt{\rho_1}+\sqrt{\rho_g}}\right)$
We_1	Weber number ($We_1 = \rho_g(v_g - v_1)^2 D_1/\sigma$)

Greek symbols

ν	kinematic viscosity (m^2/s)
σ	surface tension (N/m)
ρ_g	gas density (kg/m^3)
ρ_1	liquid density (kg/m^3)
η_1	liquid viscosity (Pa s or mPa s)
λ_1	wavelength of waves produced in the exit of nozzle ($\lambda_1 = \frac{2Cb_g}{\sqrt{Re_g}}\frac{\sqrt{\rho_1}}{\sqrt{\rho_g}}$)
$\dot{\gamma}$	flow rate (s^{-1}) ($\dot{\gamma} = \frac{v_c}{\lambda_1}$)

Subscripts

g	gas
l	liquid

solution, with diffusion of the ions into the polysaccharide droplet. Both techniques can produce microgels in a large range of sizes, depending on the conditions employed in the process, but the methodology of emulsion formation requires an additional process step to remove the oil phase from the microgels (Burey et al., 2008).

Thus, the purpose of this work was to study the production of microgels composed of κ-carrageenan, with or without sodium caseinate, by extrusion into a salt solution, examining the influence of the process parameters on the morphology, the stability of microgels and rheological behavior of the microgel suspensions.

2. Materials and methods

2.1. Material

The ingredients used to prepare the systems were κ-carrageenan, gently supplied by CPKelco (Atlanta, USA), casein (Sigma–Aldrich Co., St. Louis, USA) and analytical-grade potassium chloride (Labsynth, Diadema, Brazil). The κ-carrageenan powder was characterized by atomic absorption (AA) spectroscopy, and the following composition of ions was obtained: Na = 1.32%, Ca = 2.54% and K = 1.83% (w/w).

2.2. Preparation of the stock solutions

The polysaccharide stock solution (3% w/v) was prepared by dissolving κ-carrageenan in deionized water, followed by heat treatment at 90 °C for 60 min with magnetic stirring and subsequent cooling to 50 °C. Sodium caseinate (Na-CN) stock solution (6% w/v) was prepared by dispersing casein in deionized water using a magnetic stirrer, and maintaining the pH constantly adjusted to 7.0 with 10 mol/L NaOH. After this, the protein solution was heated to 50 °C and the two stock solutions were diluted and mixed to prepare the microgels. The temperature of the solutions was maintained at 50 °C using a thermostatic bath filled with distilled water. Pure microgels were obtained from the κ-carrageenan solution, whilst the mixed microgels were produced from the mixture of the κ-carrageenan and sodium caseinate solutions.

2.3. Visual phase diagrams

Visual κ-carrageenan/KCl and κ-carrageenan/Na-CN/KCl phase diagrams were constructed in order to establish the appropriate concentrations of salt and biopolymers for gel formation. In order to construct the visual phase diagrams, the biopolymer stock solutions were diluted to the desired concentration at 50 °C, and 4 mL of each solution mixed with 4 mL of each KCl solution. For the κ-carrageenan/KCl phase diagram, the polysaccharide concentration varied between 0.5% and 3% (w/v) and the KCl concentration from 0.1% to 3% (w/v). For the κ-carrageenan/Na-CN/KCl diagram, the same salt concentration was used and the κ-carrageenan/Na-CN ratio varied between 0.2 and 5.0, with a total biopolymer concentration (protein + polysaccharide) of 3% (w/v). These mixtures were stirred and placed into a temperature – controlled chamber (model TE-391, Tecnal, Brazil) at 10 °C. After 24 h of storage, the gel formation was visually evaluated. From these data it was possible to construct the sol–gel transition diagrams and to set up some of the conditions for microgel preparation.

2.4. Microgels

2.4.1. Microgel production

The microgels were produced by the extrusion method using pure aqueous κ-carrageenan solutions and mixtures of κ-carrageenan and sodium caseinate solutions (Table 1). The surface tension of these solutions was measured using a Sigma 70 tensiometer (KSV Instruments, Finland) at 50 °C and the values are shown in Table 1. The viscosity of the biopolymer solutions was determined according to Section 2.4.3.3.

In order to produce the microgels, hot biopolymer solutions (50 °C) were extruded from an atomizer nozzle (1.2 mm diameter) into a 0.5% (w/v) KCl solution (concentration determined from the visual phase diagrams) at room temperature. The height from the atomizer nozzle to the KCl solution (Fig. 1A) was fixed at H = 200 mm, which is greater than the distance for the completion of atomization (~50 mm) (Aliseda et al., 2008). The feed flow rate varied between 0.3 and 1.0 L/h, while the compressed air flow rate at the nozzle varied from 0.3 to 1.2 m^3/h. The gelled particles were

Table 1
Biopolymer concentration and surface tension at 50 °C of the fluids used to prepare the microgels.

	κ-Carrageenan (%)	Na-CN (%)	Surface tension (mN/m)
Pure κ-carrageenan solutions			
	0.5		58.79 ± 0.63[A]
	1.0		56.98 ± 0.81[B]
	2.0		58.16 ± 1.26[A]
	3.0		63.02 ± 1.32[C]
Mixed κ-carrageenan – Na-CN solutions			
κ-Carrageenan/Na-CN ratio	κ-Carrageenan (%)	Na-CN (%)	Surface tension (mN/m)
0.2	0.5	2.5	43.32 ± 0.59[D]
0.5	1.0	2.0	44.73 ± 0.42[E]
1.0	1.5	1.5	47.48 ± 0.19[F]
2.0	2.0	1.0	46.99 ± 0.22[F]
5.0	2.5	0.5	47.50 ± 0.20[F]

Different letters indicate significant differences at $p < 0.05$ in the same column.

maintained in the salt solution for 30 min (Chan et al., 2009) and then filtered through a sieve with opening of 0.053 mm. The microgels were stored at 10 °C and the microstructure and rheology of their suspensions evaluated.

2.4.2. Dimensionless numbers of the atomization process

The configuration of the atomizer nozzle used in this work is schematically shown in Fig. 1B. It consists of a round liquid jet surrounded by a co-flowing annular gas stream. The diameter of the liquid jet was $D_l = 1.2$ mm and the gas nozzle exit diameter was $D_g = 3.0$ mm. The liquid and gas velocities (v_l and v_g) at the exit of the nozzle were calculated from the ratio between their respective volume flow rates ($\dot{\gamma}_l$ and $\dot{\gamma}_g$) and exit areas (A_l and A_g).

The Reynolds numbers of the gas (Re_g) and liquid layers ($Re_{\lambda l}$) can be calculated from Eqs. (1) and (2), respectively.

$$Re_g = \frac{v_g b_g}{\nu_g} \tag{1}$$

$$Re_{\lambda l} = \frac{(v_c - v_l)\lambda_l}{\nu_l} \tag{2}$$

where ν_l and ν_g are kinematic viscosities (ratio between the liquid dynamic viscosity and its density) of the liquid and gas (m^2/s), respectively, v_c is the velocity of the waves produced in the exit of nozzle $\left(v_c = \left(\frac{\sqrt{\rho_l}v_l + \sqrt{\rho_g}v_g}{\sqrt{\rho_l}+\sqrt{\rho_g}}\right)\right)$ and λ_l is the wavelength $\left(\lambda_l \approx \frac{2Cb_g}{\sqrt{Re_g}}\frac{\sqrt{\rho_l}}{\sqrt{\rho_g}}\right)$, where C is the coefficient of proportionality that depends on the nozzle design, and was considered as 1.2 (Varga et al., 2003), ρ_l is the liquid density (kg/m^3), ρ_g is the gas density (kg/m^3) and b_g is the thickness of the gas layer ($b_g = D_g - D_l$).

Biopolymeric solutions can present non-Newtonian behavior depending on their concentration, which means that the viscosity values vary with the shear rate. The shear rate is a consequence of the hydrodynamics and in the atomization process can be estimated using Eq. (3) (Aliseda et al., 2008).

$$\dot{\gamma} = \frac{v_c}{\lambda_l} \tag{3}$$

The Ohnesorge number (Oh), which relates the liquid viscosity to the surface tension, and the Weber number (We_l) that defines the ratio between the destabilizing dynamic pressure forces exerted by the gas on the liquid and the confining forces associated with the surface tension (Varga et al., 2003), can be determined by Eqs. (4) and (5), respectively.

$$Oh = \frac{\eta_l}{\sqrt{\rho_l \sigma D_l}} \tag{4}$$

$$We_l = \frac{\rho_g (v_g - v_l)^2 D_l}{\sigma} \tag{5}$$

where η_l is the liquid viscosity (Pa s) at the process shear rate and σ is the surface tension (N/m).

2.4.3. Microgel evaluation

2.4.3.1. Optical microscopy and analysis of the microgel morphology. The morphology of the microgels was evaluated by optical microscopy using a Scope A1 microscope (Carl Zeiss, Germany) with a 10× objective lens. For this, the microgels were stained with methylene blue, poured onto microscope slides and carefully covered with glass cover slips. At least 10 images were obtained for each sample.

The particle size distribution (PSD) and shape of the microgels were determined from image analysis using the public domain software Image J v1.36b (http://www.rsb.info.nih.gov/ij/). Measurements of the maximum (F_{max}) and minimum (F_{min}) Feret diameters were carried out for each particle, with a total of 400 particles per sample. The aspect ratio (AR) was obtained from the relation between F_{max} and F_{min} (Eq. (6)). The mean particle size ($\bar{d}$) was determined from the equivalent sphere area (Eq. (7)), considering that the particles had an ellipsoidal shape (Pabst et al., 2006), and the volume-surface mean diameter (d_{32}) was calculated (Eq. (8)) in order to compare the size between different microgels.

$$AR = \frac{F_{max}}{F_{min}} \tag{6}$$

$$\bar{d} = \sqrt{F_{max} \cdot F_{min}} \tag{7}$$

$$d_{32} = \frac{\sum n_i d_i^3}{\sum n_i d_i^2} \tag{8}$$

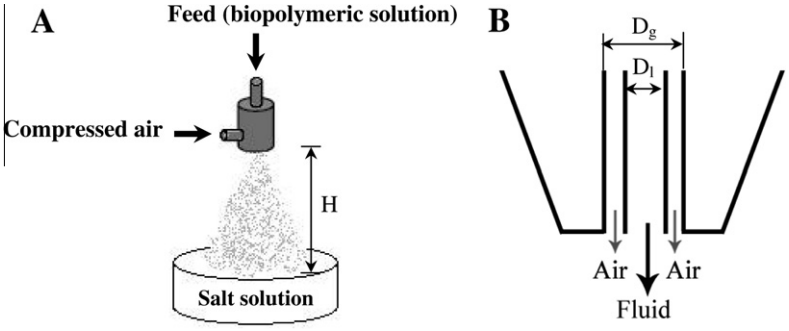

Fig. 1. (A) Extrusion formation of microgels and (B) atomizer nozzle. H = height from the atomizer nozzle to the salt solution, D_l = diameter of the fluid nozzle exit and D_g = diameter of gas nozzle exit.

The particle size distribution of the microgels was determined from the mean equivalent diameter ($\bar{d}$) and a log-normal frequency distribution function (Eq. (9)) (McClements, 2005).

$$f(\ln \bar{d}) = \frac{1}{\ln \mathrm{SD}\sqrt{2\pi}} \exp\left[\frac{-(\ln \bar{d} - \ln \bar{d}_g)^2}{2\ln^2 \mathrm{SD}}\right] \quad (9)$$

where $\bar{d}_g$ and SD are the geometric mean and the standard deviation of the geometric mean, as given by Eqs. (10) and (11), respectively.

$$\bar{d}_g = \frac{\sum n_i \bar{d}_i}{N} \quad (10)$$

$$\mathrm{SD} = \sqrt{\frac{\sum n_i (\bar{d}_i - \bar{d}_g)^2}{N}} \quad (11)$$

where n_i is the number of particles with diameter $\bar{d}_i$ and N is the total number of particles.

2.4.3.2. Evaluation of microgel stability in water and salt solutions. Microgels composed only of 3% (w/v) κ-carrageenan were used to evaluate their stability in aqueous solutions. Suspensions were prepared by dispersing 10% (v/v) microgels in deionized water or in the different potassium chloride solutions at concentrations of 0.05%, 0.1%, 0.5%, 1%, 5% and 10% (w/v). The microgel suspensions were stored at room temperature and aliquots were collected after pre-determined time periods (5, 10, 20 and 60 min) and observed using an optical microscope. The stability was determined by modification of size and shape of microgels within the evaluated period.

2.4.3.3. Rheological measurements of the suspensions. The rheological properties of the microgel suspensions (20%, 40% and 60% particles (w/w) dispersed in 10% w/v KCl solutions were evaluated. A modular compact rheometer Physica MCR301 (Anton Paar, Austria) with a rough parallel plate geometry (50 mm) and 2 mm gap was used for the measurements. Flow curves were obtained by an up-down-up steps program with the shear rate varying between 0 and 300 s^{-1}. All measurements were performed in triplicate at 25 °C. Flow curves of biopolymeric solutions were obtained under the same conditions as the suspensions.

2.5. Statistical analysis

Significant differences were determined by the Tukey test. Statistical analyses were performed using the software STATISTICA 5.5 (Statsoft, Inc., Tulsa, USA) and the level of confidence was 95%.

3. Results and discussion

3.1. Visual phase diagrams

Fig. 2A and B show the visual phase diagrams obtained for κ-carrageenan and κ-carrageenan/Na-CN, respectively, in the presence of KCl. The phase diagrams were divided into two regions (sol and gel). It is evident from Fig. 2 that κ-carrageenan gel formation occurred at a critical value of KCl concentration of approximately 0.5% (w/v) or above, whilst below this value, a coil–helix transition could take place but without helix aggregation or gelation (Núñez-Santiago and Tecante, 2007). An exception was the 3% (w/v) κ-carrageenan sample, which formed a gel without the need for salt addition. At 0.5% and 1% (w/v) KCl, the systems composed of pure κ-carrageenan (Fig. 2A) gelled at all the biopolymer concentrations (between 0.5% and 3% w/v polysaccharide). However, the systems containing 0.5% (w/v) polysaccharide at higher salt concentrations (2% and 3% w/v) did not form gels. This result is consistent with the findings of Lai et al. (2000), who verified maximum elasticity during gelation (indicated by G' and tan δ) at salt concentrations around 1% (w/w) KCl (0.1–0.2 M).

κ-Carrageenan/Na-CN/KCl (Fig. 2B) mixed systems showed gel formation for salt concentrations between 0.5% and 2% (w/v) and κ-carrageenan/Na-CN ratios above 0.5, showing the relevance of the presence of κ-carrageenan in gel formation. In particular, for 0.5% (w/v) KCl, all the mixed κ-carrageenan–sodium caseinate solutions showed gel formation. In contrast, the 3% (w/v) KCl solution did not promote gel formation for any of the systems studied. We can speculate that the elevated salt concentration could lead to a disordered aggregation of protein and polysaccharide molecules, with expulsion of water (syneresis) and without formation of a three-dimensional network. Comparing Fig. 2A and B, it could be seen that both the pure and mixed systems formed gels when the κ-carrageenan concentration was above 0.5% (w/v), which means that this was the minimum biopolymer concentration to be used. Similar result was reported by Şen and Erboz (2010), who observed formation of gel structure of κ-carrageenan at concentrations above 0.7% (w/v). Since most of the systems showed gel formation when mixed in the 0.5% (w/v) KCl solution, this salt concentration was chosen to prepare the microgels.

3.2. Microgels

The main factors determining the final diameter of the microgels are: (1) biopolymer flow rate, (2) compressed air flow rate at the atomizer nozzle and (3) microgel composition (Herrero et al.,

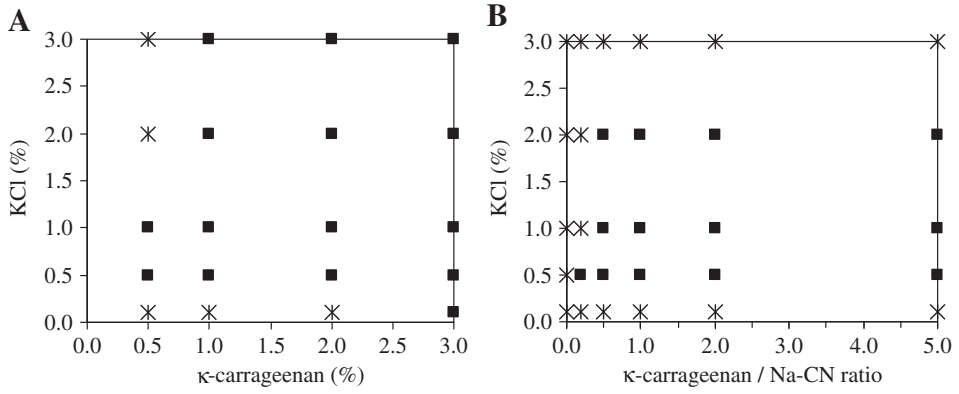

Fig. 2. Visual phase diagram of (A) κ-carrageenan/KCl systems and (B) κ-carrageenan/Na-CN/KCl systems (total biopolymers concentration of 3% w/v). (■) Gel points and (✳) sol points.

2006). The influence of each factor was studied and the results are detailed below.

3.2.1. Effect of the feed flow rate

In order to evaluate the influence of feed flow rate on the final morphology of the microgels, the systems were produced at a fixed κ-carrageenan concentration of 2% (w/v), compressed air flow rate of 1.2 m^3/h (maximum value), and with a feed flow rate ranging from 0.3 to 1 L/h. Fig. 3 illustrates the particle size distribution and morphology of the microgels produced under these conditions.

Fig. 3 shows that the mean diameter of the microgels increased with increase in the feed flow rate between 0.3 and 0.5 L/h, becoming almost constant between 0.5 and 1.0 L/h. The principle of atomization consists in the formation of a liquid film exiting the nozzle, which is exposed to an air flow moving at high velocity. The contact between liquid and air produces waves (primary instability) that disintegrate into fragments when the wave amplitude reaches a critical value. The fragments rapidly contract into unstable ligaments under the action of surface tension, which break up into droplets (Herrero et al., 2006; Rizk and Lefebvre, 1980). An increase in feed flow rate leads to the formation of thicker films of liquid at the nozzle, which break down into bigger droplets (Herrero et al., 2006; Rizk and Lefebvre, 1980). There are many dimensionless parameters that influence the breakup process when using coaxial atomizer nozzles (Varga et al., 2003). The evaluation of the dimensionless parameters ($Re_{\lambda l}$ and We) involved in the atomization process showed little differences between the distinct conditions (results not shown), confirming the limited influence of this range of feed flow rate on the production of the microgels. The polydispersity of the microgels (σ_g) followed the same tendency as the mean diameter, and the aspect ratio of the microgels showed no significant differences with the change in feed flow rate. Thus, a feed flow rate of 0.3 L/h was chosen in order to produce microgels with smaller diameters and polydispersity.

3.2.2. Effect of compressed air flow rate

The effect of the air flow rate (0.3, 0.6, 0.9 and 1.2 m^3/h) on the atomizer nozzle was evaluated using fixed values for the κ-carrageenan concentration (2% w/v) and feed flow rate (0.3 L/h). As shown in Fig. 4A, the microgel produced at the lowest compressed air flow rate (0.3 m^3/h) showed a spherical shape and mean diameter (d_{32}) of around 1.5 mm, which is larger than the atomizer nozzle diameter (1.2 mm). In this case, the force exerted by the compressed air was probably not sufficient to overcome the surface tension force, and thus the droplets were formed when the gravity force on the liquid exceeded the surface tension force (Lefebvre, 1989), hindering the breakup of the droplets into smaller ones. The increase in the compressed air flow rate from 0.3 to 1.2 m^3/h led to a gradual reduction in the mean diameter of the microgels (Fig. 4E) and an increase in the aspect ratio and polydispersity (Fig. 4B–D). The influence of the compressed air flow rate on the particle size can once more be explained by the mechanism of film disruption and droplet formation. With the increase in compressed air flow rate, the liquid film disintegrated earlier and the ligaments were formed nearer the nozzle. These ligaments tended to be thinner and shorter, disintegrating into smaller droplets (Rizk and Lefebvre, 1980).

Table 2 shows the shear rate at the atomizer nozzle, the apparent viscosity of the biopolymer solutions and the dimensionless parameters calculated for the different conditions of compressed air flow rate. All the parameters were highly influenced by the change in compressed air flow rate. The shear rate at the outlet from the nozzle was estimated to be higher than the range tested experimentally (300 s^{-1}). Thus the viscosity of the biopolymer solution at the shear rate of atomization was estimated from the fitted equation (power law or Herschel Bulkley), and this value was used to calculate the dimensionless parameters. The Reynolds number of the gas was highly influenced by the air flow rate, showing an increase in the turbulence at higher values of flow rate. The

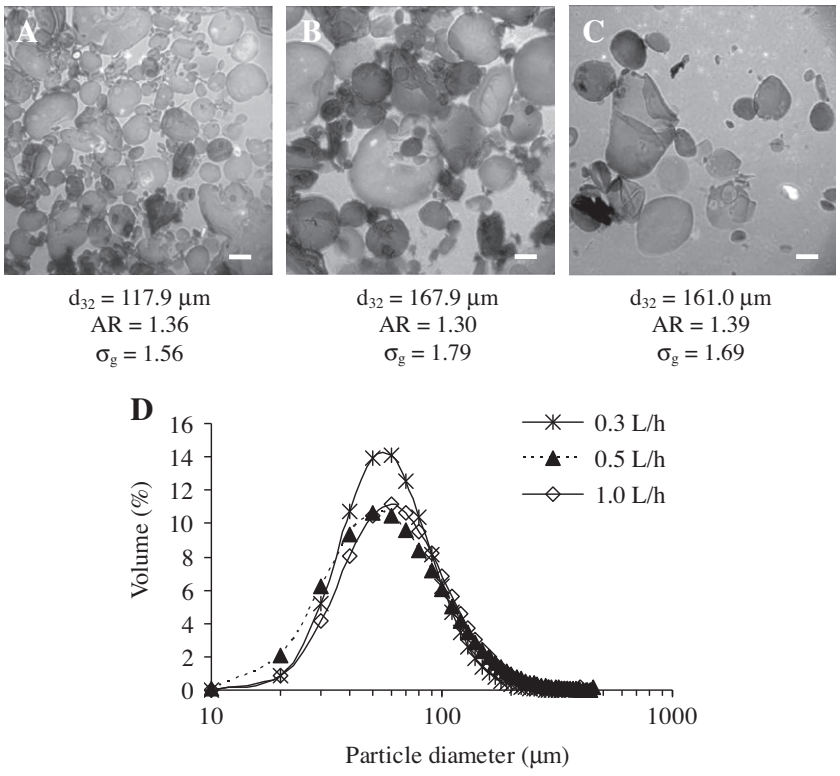

Fig. 3. Particle size distribution (Fig. 3D) and microscopic images of 2% (w/v) κ-carrageenan microgels produced at a fixed compressed air flow rate and different feed flow rates: (A) 0.3 L/h, (B) 0.5 L/h and (C) 1.0 L/h. Scale bar = 100 μm.

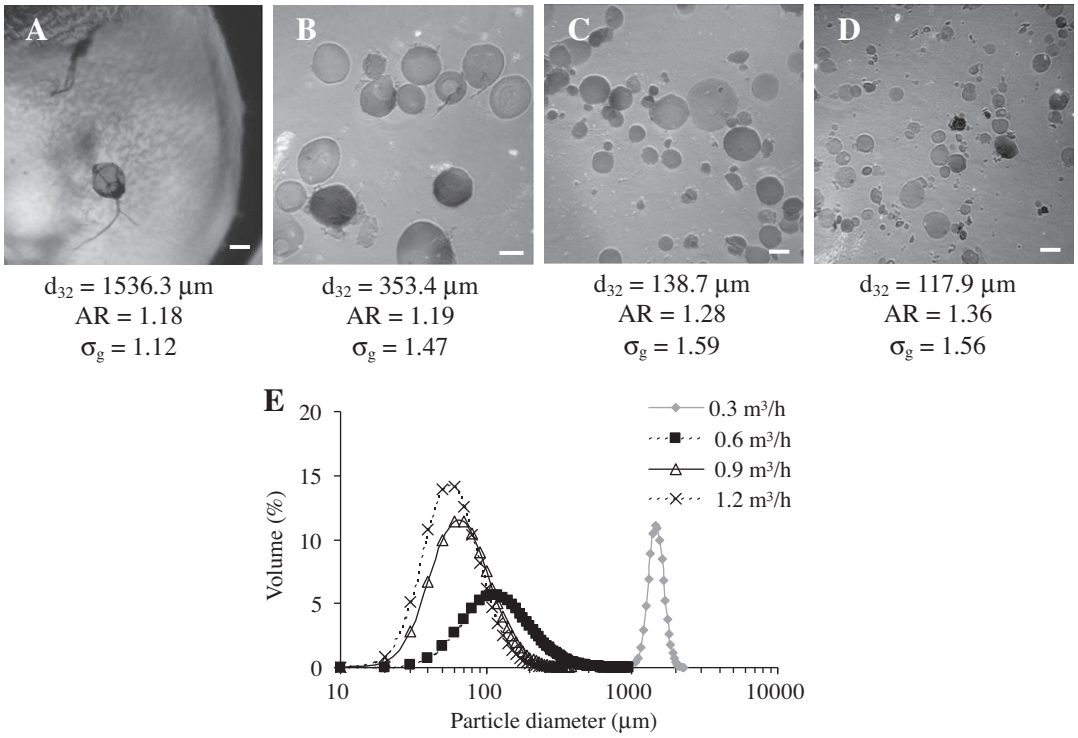

Fig. 4. Micrographs of 2% (w/v) κ-carrageenan microgels produced at a fixed feed flow rate (0.3 L/h) and different compressed air flow rates: (A) 0.3 m^3/h, (B) 0.6 m^3/h, (C) 0.9 m^3/h and (D) 1.2 m^3/h. (E) Particle size distribution of these microgels. Scale bar = 100 μm.

Table 2
Shear rate, solution viscosity and dimensionless parameters of the experiments at different compressed air flow rates.

Air flow rate (m^3/h)	$\dot{\gamma}$ (s^{-1})	η_1^*[a] (mPa s)	Re_g	$Re_{\lambda l}$	Oh	We_l
0.3	927	37.1 ± 0.5	5275	20.8	0.14	15
0.6	2519	33.8 ± 0.4	10,549	32.4	0.12	62
0.9	4565	32.0 ± 0.3	15,824	41.9	0.12	139
1.2	6981	30.8 ± 0.3	21,098	50.4	0.11	247

[a] Viscosity calculated at the shear rate of the extrusion process.

Reynolds number of the liquid layer also increased with the air flow rate and was higher than ~10 in all situations, which is the condition necessary to develop the primary instability (Aliseda et al., 2008) and consequently droplet breakup. However, the value of $Re_{\lambda l}$ close to 10 in the lowest air flow rate reinforced the assumption that the compressed air was not efficient in the break-up of the droplets under this condition. The Ohnesorge number was only slightly influenced by the air flow rate, because the viscosity at the different shear rates was very similar. This dimensionless number can be related to the microgel sphericity (Chan et al., 2009), which explains the increase of aspect ratio with the increment of compressed air flow rate (lower Oh). The Weber number increased at higher values of air flow rate (in the same way as the Reynolds number), indicating that the waves produced at the

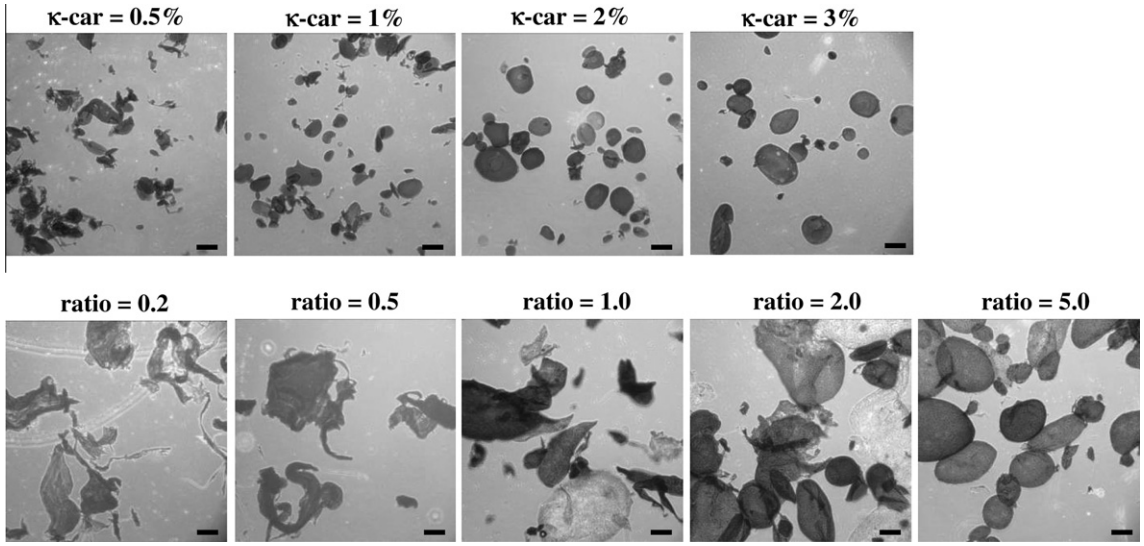

Fig. 5. Microstructure of the microgels composed of κ-carrageenan (κ-car) and the mixture between κ-carrageenan and Na-CN (different ratios). Scale bar = 100 μm.

Table 3
Mean droplet diameter and aspect ratio of the microgels prepared from different biopolymer solutions and the dimensionless atomization process parameters.

	d_{32} (m)	AR	η_l[a] (mPa s)	Re_g	$Re_{\lambda l}$	Oh	We_l
κ-Carrageenan (%)							
0.5	83.7 ± 14.0	1.68 ± 0.13	5.4 ± 0.1	21,098	288	0.02	244
1.0	89.9 ± 14.1	1.47 ± 0.04	11.1 ± 0.0	21,098	140	0.04	252
2.0	136.3 ± 25.0	1.36 ± 0.05	30.8 ± 0.3	21,098	50	0.11	247
3.0	159.6 ± 17.6	1.33 ± 0.05	66.1 ± 2.1	21,098	23	0.23	228
κ-Carrageenan/Na-CN ratio							
0.2	142.8 ± 29.04	1.90 ± 0.12	6.1 ± 0.1	21,098	255	0.03	331
0.5	161.7 ± 31.8	1.84 ± 0.10	14.5 ± 0.2	21,098	107	0.06	321
1.0	165.9 ± 40.4	1.86 ± 0.07	24.7 ± 0.2	21,098	63	0.10	302
2.0	224.1 ± 33.8	1.75 ± 0.16	33.3 ± 0.1	21,098	47	0.14	305
5.0	235.1 ± 46.0	1.64 ± 0.13	49.7 ± 0.3	21,098	31	0.20	302

[a] Viscosity calculated at the shear rate of the extrusion process.

primary instability grew more quickly (Aliseda et al., 2008), favoring the production of smaller droplets.

From these results, a compressed air flow rate of 1.2 m^3/h was chosen to produce the microgels in the following steps of this study.

3.2.3. Evaluation of the microgel composition

For the evaluation of the composition on the microgel morphology, extrusion was carried out at a constant feed flow rate (0.3 L/h) and compressed air flow rate (1.2 m^3/h) as previously determined. Fig. 5 shows the microstructure of the pure (0.5%, 1%, 2% and 3% κ-carrageenan) and mixed (κ-carrageenan/Na-CN ratios of 0.2, 0.5, 1.0, 2.0 and 5.0, with total biopolymer concentration of 3% w/v) microgels, from which the considerable dependence of the particle morphology on the biopolymer composition can be verified.

The results obtained for droplet diameter and aspect ratio (Table 3) indicated that an increase in the κ-carrageenan concentration and the κ-carrageenan/Na-CN ratio led to the formation of larger and more spherical particles. The increased size of the droplets could be related to the greater density of the biopolymers,

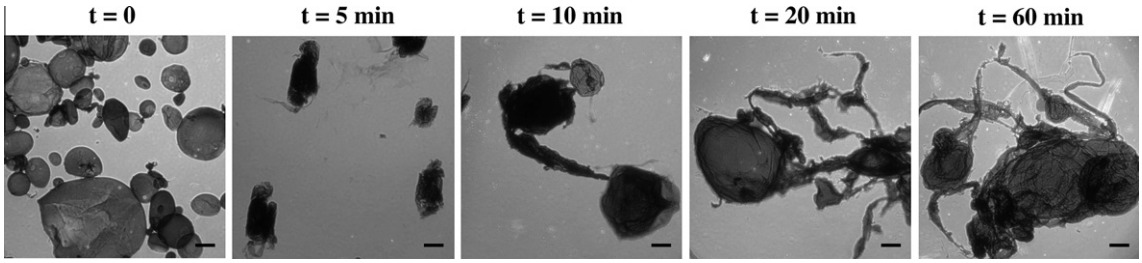

Fig. 6. Evaluation of the stability of 3% (w/v) κ-carrageenan microgels dispersed in deionized water, where *t* is the time of incubation. Scale bar = 100 μm.

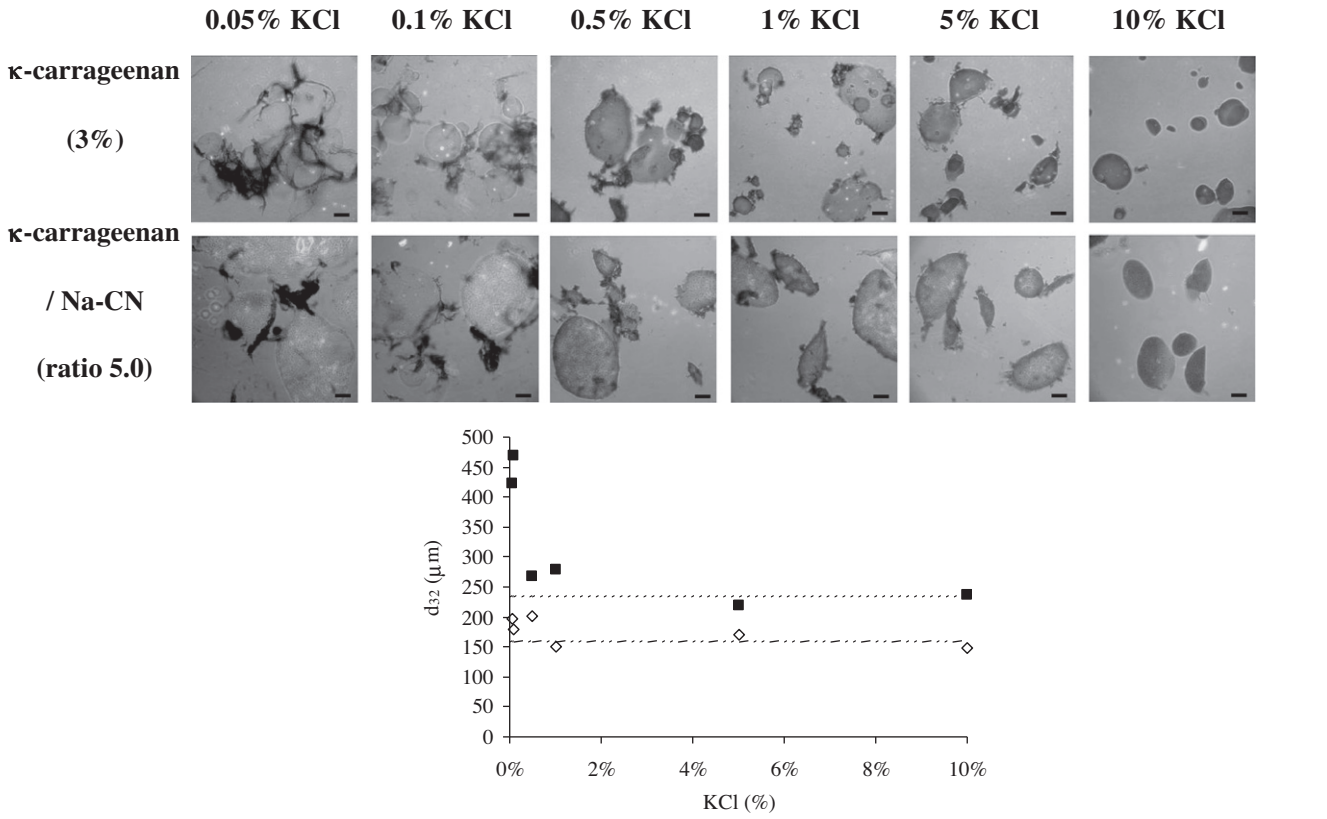

Fig. 7. Micrographs and mean particle diameter (d_{32}) of the microgels dispersed in different salt solutions after 1 h of incubation. Scale bar = 100 μm. Microgels of 3% κ-carrageenan (◇) dispersed in KCl solutions and (– – – –) before dilution; microgels of κ-carrageenan/Na-CN ratio of 5.0 (■) dispersed in KCl solutions and (- - - - -) before dilution.

which resulted in thicker films at the nozzle and consequently in an increase in droplet diameter (Rizk and Lefebvre, 1980). On the other hand, the more spherical shape could be associated with the higher surface tension and viscosity of the biopolymeric solutions (Tables 1 and 3) (Chan et al., 2009).

The comparison between the pure and mixed microgels showed that the systems containing sodium caseinate presented higher values for the diameter and aspect ratio than the pure systems made with biopolymer solutions of similar viscosity i.e., the addition of protein led to the formation of larger and less spherical particles. This probably occurred because the addition of protein led to the formation of a more porous biopolymeric matrix due to the weak or even repulsive interactions between the protein and polysaccharide, especially for κ-carrageenan/Na-CN ratios of 2.0 and

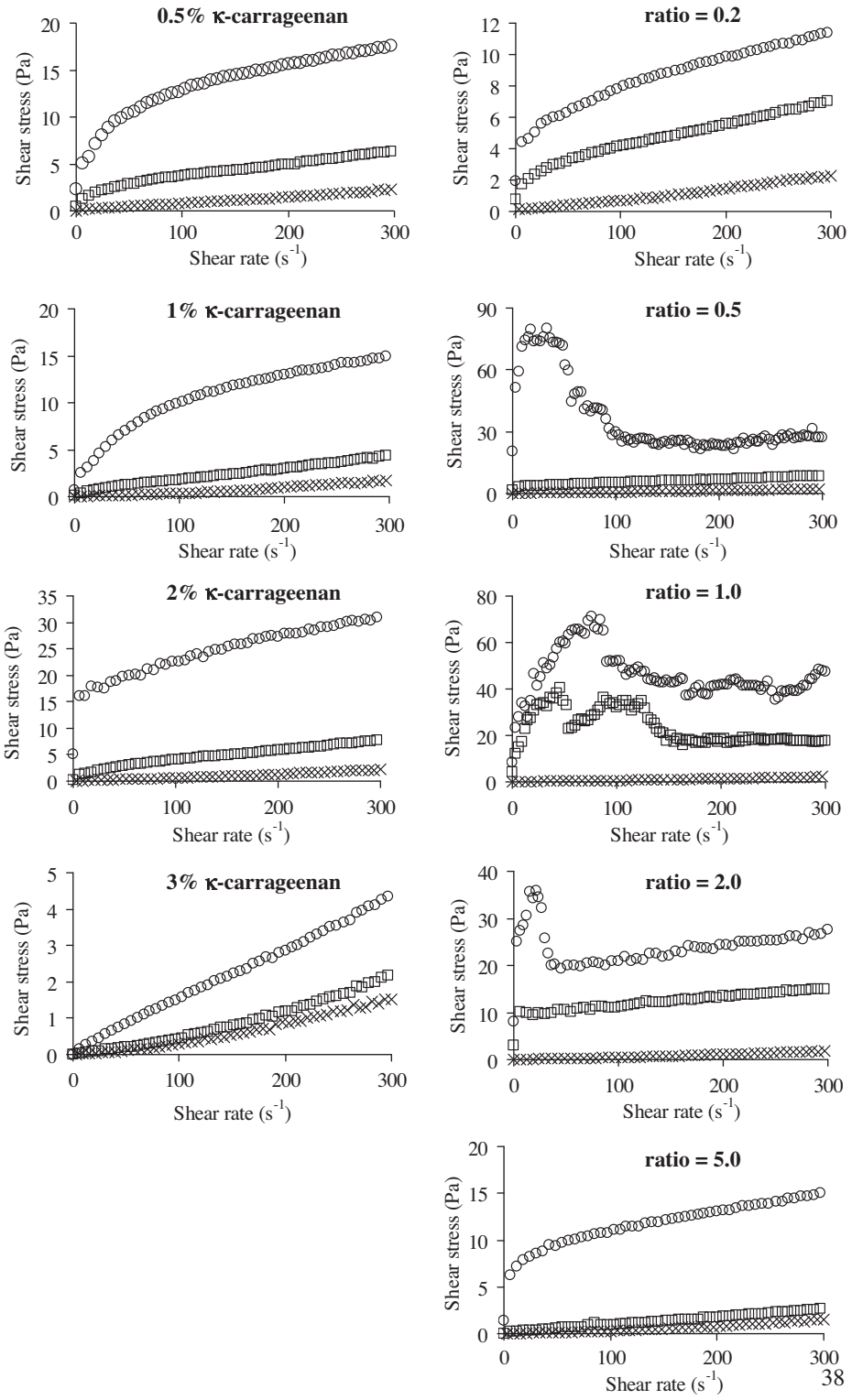

Fig. 8. Flow curves of κ-carrageenan and κ-carrageenan/Na-CN microgel suspensions after elimination of time dependence. Volume fraction: (×) 20%, (□) 40% and (○) 60%.

5.0 (excess of polysaccharide), leading to an increase in particle diameter. Nono et al. (in press) also studied the interaction between κ-carrageenan and sodium caseinate and verified a process of phase separation above a critical concentration of either κ-carrageenan or Na-CN. The difference in morphology of the microgels probably occurred due to the lower values of surface tension of the mixed solutions, which allowed the droplets to become more irregular before gelation.

Table 3 shows the evaluation of the dimensionless parameters involved in the atomization process, as well as the estimated viscosity of the biopolymer solutions used to calculate these parameters. The values for viscosity were estimated from the flow curves of the solutions, using a shear rate of 6980 s^{-1} as determined from Eq. (3). These data showed that the Reynolds number of the liquid layer decreased with increases in the apparent viscosity, but in all cases the $Re_{\lambda l}$ was higher than 10 (condition necessary for droplet breakup). On the other hand, the Ohnesorge number increased, demonstrating the greater influence of liquid viscosity in relation to surface tension (Aliseda et al., 2008) and leading to the formation of more spherical particles (Chan et al., 2009). As the process parameters (v_g, v_l and D_l) were maintained constant during the experiments, the Weber number was mainly related to the surface tension of the biopolymer solutions (Table 1), being lower for the pure polysaccharide solutions (higher σ values) and higher for the mixed solutions (lower σ values). Since higher values for the We number should lead to the formation of smaller droplets (Aliseda et al., 2008), the mixed solutions should produce smaller particles than the pure ones. However, the incompatibility or repulsive interactions between the κ-carrageenan and the sodium caseinate, probably led to the production of larger microgels.

3.3. Evaluation of microgel stability

The systems composed of 3% (w/v) κ-carrageenan and κ-carrageenan/Na-CN ratio of 5.0 were used in the evaluation of particle stability in water and salt solutions, because of their more spherical shape as compared to the other pure and mixed microgels, respectively. The micrographs of the 3% (w/v) κ-carrageenan microgels dispersed in deionized water (Fig. 6) showed that the particles were loosing their shape and seemed to swell during incubation. In this way, it was concluded that this type of microgel was not stable in deionized water.

The evaluation of microgel stability in salt solutions was carried out using different concentrations of KCl (0.05%, 0.1%, 0.5%, 1%, 5% and 10%). Fig. 7 shows the photos of pure (3% κ-carrageenan) and mixed (κ-carrageenan/Na-CN ratio of 5.0) microgels dispersed in the salt solutions after 1 h of incubation, with the mean particle diameter (d_{32}). At low salt concentrations of up to 0.5% KCl, the microgels lost their shape and merged into each other. An increase in salt concentration (>1% KCl) avoided the fusion of the particles, but they were still quite swollen and with an irregular shape. Only from KCl concentrations above 5%, the microgels became more spherical and at 10% KCl they were similar to the microgels with no dilution. A comparison of the values obtained for mean diameter indicated that an increase in KCl concentration led to a significant reduction in diameter of the microgels. Covalently cross-linked microgels of κ-carrageenan (Ellis et al., 2009), alginate (Moe et al., 1993) and gellan gum (Annaka et al., 2000) showed the same tendency to increase the particle size with reduction in salt concentration, but the covalent bonds of the cross-linked microgels favored maintenance of the spherical shape. Thus, the microgels probably lost their shape due to the higher affinity of KCl for the water, i.e., the salt tended to migrate to the water, destabilizing the particles.

The difference in diameter of the microgels with salt concentration can be explained by the Donnan equilibrium, in which the difference in ionic concentration between the inside and outside of the microgel should be reduced when salt in the surrounding medium is increased (Ellis et al., 2009). At lower salt contents, the ion concentration inside the particles is higher than in the surrounding solution, so in order to minimize this disequilibrium, water penetrates into the microgels, making them swell. On the other hand, with increases in the salt concentration of the surrounding solution, the opposite effect occurs, leading to shrinkage of the particles (Keppeler et al., 2009; Ellis et al., 2009). Comparing the results obtained for the morphology and diameter of the microgels dispersed in different salt solutions, the 10% KCl solution was chosen as the dispersing medium for the study of suspension rheology (Section 3.4).

3.4. Evaluation of the rheology of the microgel suspensions

Fig. 8 illustrates the flow curves of the microgels dispersed in 10% KCl solutions. The curves of the pure microgel (κ-carrageenan) suspensions fitted the power law model well, while those of the mixed microgels (κ-carrageenan–sodium caseinate) were best fitted to the Herschel–Bulkley (HB) model (results not shown). The yield stress (σ_o) observed in the mixed suspensions indicated greater interaction between the microgels, probably leading to the formation of an interconnected structure (Channell and Zukoski, 1997). In addition, most of the samples did not show thixotropy, this behavior only being observed for the more concentrated suspensions (60%) of more irregular microgels (higher AR). Some curves could not be fitted to any rheological model (Fig. 8),

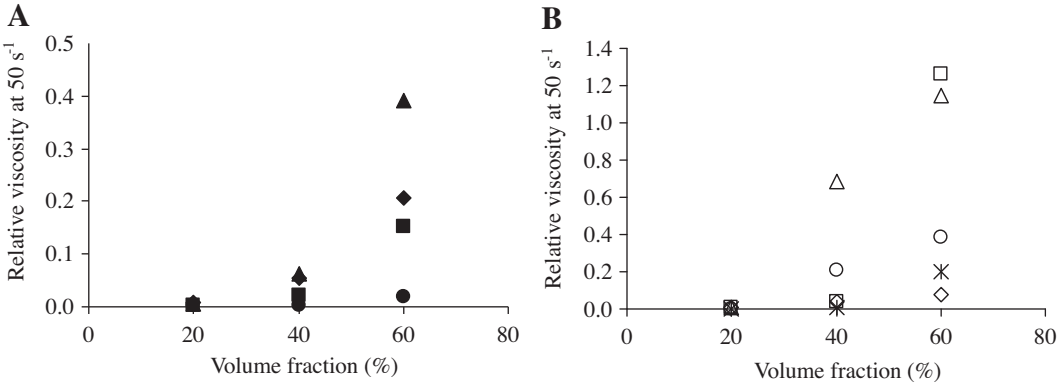

Fig. 9. Relative viscosity of κ-carrageenan and κ-carrageenan/Na-CN microgel suspensions at 50 s^{-1}. (A) Pure microgels: (♦) 0.5%, (■) 1%, (▲) 2% and (●) 3% κ-carrageenan; and (B) mixed microgels: (◇) 0.2, (□) 0.5, (△) 1.0, (○) 2.0 and (✳) 5.0 κ-carrageenan/Na-CN ratio.

even after three sweeps of stress–shear rate performed to eliminate time dependence, and presented an overshoot characteristic of more complex structures. A particle network probably formed and reformed during the application of shear, which only occurred for the more concentrated suspensions of mixed microgels, especially with intermediate κ-carrageenan/Na-CN ratios. This can be explained by the morphology of the microgels (larger diameter and mainly irregular shape) (Table 3) and also by the interaction between protein and/or polysaccharide, favored at a ratio of 1.0.

The values for relative viscosity (apparent viscosity at 50 s^{-1}/ continuous phase viscosity) were evaluated (Fig. 9) in order to compare the behavior of the suspensions at a shear rate typical of chewing (Steffe, 1996). In this case, the continuous phase viscosity was considered as the viscosity of pure water at 25 °C. In general, the suspensions of mixed microgels were more viscous than those composed of pure microgels, which could be mostly related to the shape of the particles, leading to a greater complexity of the interactions. Suspensions of irregular particles are frequently more viscous than those composed of spherical particles with the same volume fraction, which can be explained by the greater exclusion volume shown by non spherical particles, since they tend to rotate around an orbit when dispersed in solution (Lindström and Uesaka, 2008).

An increase in volume fraction led to a reduction in the flow behavior index (increase in shear-thinning behavior) (Fig. 8) and an increase in suspension viscosity for all the systems studied (Fig. 9). It is observed that the increase in shear rate in the dispersions with lower volume fraction led to greater interaction between the particles, causing an increase in dispersion viscosity or a shear-thickening behavior. As the volume fraction increased, higher shear rates led to orientation of the molecules in the direction of the flow and to breakage of the aggregates (Barnes et al., 1989) or a shear-thinning behavior. The influence of volume fraction on the rheological behavior of different suspensions was smaller for the systems containing 3% κ-carrageenan. This probably occurred because these microgels were more spherical (Table 3) than the others. On the other hand, the mixed microgel with a κ-carrageenan/Na-CN ratio of 1.0 was the system most influenced by the volume fraction (Fig. 8), which can be explained by the combination of the irregular shape (aspect ratio >>1) (Wolf et al., 2001) and greater diameter (Table 3), as well as by the electrostatic (repulsive or attractive) interactions between the caseinate and κ-carrageenan.

4. Conclusions

This work evaluated the production of κ-carrageenan and κ-carrageenan – Na-CN microgels by extrusion, using potassium chloride for gelation. The results showed that an increase in air flow rate and decrease in feed flow rate and apparent viscosity promoted the formation of the smallest microgels, which was verified by the increase of some dimensionless numbers ($Re_{\lambda l}$ and We_l). However, the aspect ratio of the particles was mainly influenced by the apparent viscosity and surface tension of the solutions, which was confirmed by the evaluation of Ohnesorge number (Oh). The biopolymer composition also influenced the microgel morphology, the mixed microgels (κ-carrageenan/Na-CN) being larger than the pure ones (κ-carrageenan), probably due to incompatibility between the protein and polysaccharide. The microgels were very unstable when dispersed in water, but they maintained their shape when diluted in solutions with a high salt content (10% KCl). The wide range in size (d_{32} between ~84 m and ~235 m) and shape (AR between 1.33 and 1.9) of the microgels led to different rheological behavior of their suspensions, from shear thinning to shear thickening with the presence (or not) of yield stress, depending on the volume fraction of the particles.

Acknowledgments

The authors are grateful to CAPES-Proex, FAPESP (2007/58017-5) and CNPq (301869/2006-5) for their financial support.

References

Adams, S., Frith, W.J., Stokes, J.R., 2004. Influence of particle modulus on the rheological properties of agar microgel suspensions. Journal of Rheology 48 (6), 1195–1213.
Aliseda, A., Hopfinger, E.J., Lasheras, J.C., Kremer, D.M., Berchielli, A., Connolly, E.K., 2008. Atomization of viscous and non-newtonian liquids by a coaxial, high-speed gas jet. Experiments and droplet size modeling. International Journal of Multiphase Flow 34 (2), 161–175.
Annaka, M., Ogata, Y., Nakahira, T., 2000. Swelling behavior of covalently cross-linked gellan gels. Journal of Physical Chemistry B 104 (29), 6755–6760.
Arltoft, D., Ipsen, R., Madsen, F., de Vries, J., 2007. Interactions between carrageenans and milk proteins: a microstructural and rheological study. Biomacromolecules 8 (2), 729–736.
Barnes, H.A., Hutton, J.F., Walters, K., 1989. An Introduction to Rheology. Elsevier Science Publishers, Amsterdam.
Belyakova, L.E., Antipova, A.S., Semenova, M.G., Dickinson, E., Merino, L.M., Tsapkina, E.N., 2003. Effect of sucrose on molecular and interaction parameters of sodium caseinate in aqueous solution: relationship to protein gelation. Colloids and Surfaces B: Biointerfaces 31 (1–4), 31–46.
Blandino, A., Macias, M., Cantero, D., 1999. Formation of calcium alginate gel capsules: influence of sodium alginate and $CaCl_2$ concentration on gelation kinetics. Journal of Bioscience and Bioengineering 88 (6), 686–689.
Bourriot, S., Garnier, C., Doublier, J.-L., 1999. Micellar-casein – κ-carrageenan mixtures I. Phase separation and ultrastructure. Carbohydrate Polymers 40 (2), 145–157.
Burey, P., Bhandari, B.R., Howes, T., Gidley, M.J., 2008. Hydrocolloid gel particles: formation, characterization, and application. Critical Reviews in Food Science and Nutrition 48 (5), 361–377.
Chan, E.–S., Lee, B.–B., Ravindra, P., Poncelet, D., 2009. Prediction models for shape and size of ca-alginate macrobeads produced through extrusion-dripping method. Journal of Colloid and Interface Science 338 (1), 63–72.
Channell, G.M., Zukoski, C.F., 1997. Shear and compressive rheology of aggregated alumina suspensions. AIChE Journal 43 (7), 1700–1708.
Dalgleish, D.G., Morris, E.R., 1988. Interactions between carrageenans and casein micelles: electrophoretic and hydrodynamic properties of the particles. Food Hydrocolloids 2 (4), 311–320.
De Ruiter, G.A., Rudolph, B., 1997. Carrageenan biotechnology. Trends in Food Science & Technology 8 (12), 389–395.
Ellis, A., Jacquier, J.C., 2009. Manufacture of food grade κ-carrageenan microspheres. Journal of Food Engineering 94 (3–4), 316–320.
Ellis, A., Keppeler, S., Jacquier, J.C., 2009. Responsiveness of κ-carrageenan microgels to cationic surfactants and neutral salts. Carbohydrate Polymers 78 (3), 384–388.
Herrero, E.P., Martín Del Valle, E.M., Galán, M.A., 2006. Development of a new technology for the production of microcapsules based in atomization processes. Chemical Engineering Journal 117 (2), 137–142.
Hunik, J.H., Tramper, J., 1993. Large-scale production of κ-carrageenan droplets for gel-bead production: theoretical and practical limitations of size and production rate. Biotechnology Progress 9 (2), 186–192.
Imeson, A.P., 2000. Carrageenan. In: Phillips, G.O., Williams, P.A. (Eds.), Handbook of Hydrocolloids. CRC Press, Boca Raton.
Keppeler, S., Ellis, A., Jacquier, J.C., 2009. Cross-linked carrageenan beads for controlled release delivery systems. Carbohydrate Polymers 78 (4), 973–977.
Lai, V.M.F., Wong, P.A.–L., Lii, C.-Y., 2000. Effects of cation properties on sol–gel transition and gel properties of κ-carrageenan. Journal of Food Science 65 (8), 1332–1337.
Langendorff, V., Cuvelier, G., Launay, B., Parker, A., 1997. Gelation and flocculation of casein micelle/carrageenan mixtures. Food Hydrocolloids 11 (1), 35–40.
Lefebvre, A.H., 1989. Atomization and Sprays. Taylor & Francis, New York.
Lindström, S.B., Uesaka, T., 2008. Simulation of semidilute suspensions of non-Brownian fibers in shear flow. Journal of Chemical Physics 128 (2), 024901-1–024901-14.
Martin, A.H., Goff, H.D., Smith, A., Dalgleish, D.G., 2006. Immobilization of casein micelles for probing their structure and interactions with polysaccharides using scanning electron microscopy (SEM). Food Hydrocolloids 20 (6), 817–824.
McClements, D.J., 2005. Food Emulsions: Principles, Practice and Techniques. CRC Press, New York.
Meunier, V., Nicolai, T., Durand, D., 2001. Structure of aggregating κ-carrageenan fractions studied by light scattering. International Journal of Biological Macromolecules 28 (2), 157–165.
Moe, S.T., Skjak-Braek, G., Elgsaeter, A., Smidsroed, O., 1993. Swelling of covalently crosslinked alginate gels: influence of ionic solutes and nonpolar solvents. Macromolecules 26 (14), 3589–3597.

Morris, E.R., Rees, D.A., Robinson, G., 1980. Cation-specific aggregation of carrageenan helices: Domain model of polymer gel structure. Journal of Molecular Biology 138 (2), 349–362.

Nono, M., Nicolai, T., Durand, D., in press. Gel formation of mixtures of κ-carrageenan and sodium caseinate. Food Hydrocolloids, doi:10.1016/j.foodhyd.2010.07.014.

Núñez-Santiago, M.C., Tecante, A., 2007. Rheological and calorimetric study of the sol–gel transition of κ-carrageenan. Carbohydrate Polymers 69 (4), 763–773.

Oakenfull, D., Miyoshi, E., Nishinari, K., Scott, A., 1999. Rheological and thermal properties of milk gels formed with κ-carrageenan I. Sodium caseinate. Food Hydrocolloids 13 (6), 525–533.

Pabst, W., Berthold, C., Gregorová, E., 2006. Size and shape characterization of polydisperse short-fiber systems. Journal of the European Ceramic Society 26 (7), 1121–1130.

Poncelet, D., Lencki, R., Beaulieu, C., Halle, J.P., Neufeld, R.J., Fournier, A., 1992. Production of alginate beads by emulsification/internal gelation. I. Methodology. Applied Microbiology and Biotechnology 38 (1), 39–45.

Reis, C.P., Neufeld, R.J., Vilela, S., Ribeiro, A.J., Veiga, F., 2006. Review and current status of emulsion/dispersion technology using an internal gelation process for the design of alginate particles. Journal of Microencapsulation 23 (3), 245–257.

Ribeiro, K.O., Rodrigues, M.I., Sabadini, E., Cunha, R.L., 2004. Mechanical properties of acid sodium caseinate–κ-carrageenan gels: effect of co-solute addition. Food Hydrocolloids 18 (1), 71–79.

Rizk, N.K., Lefebvre, A.H., 1980. The influence of liquid film thickness on airblast atomization. Journal of Engineering for Power 102 (7), 706–710.

Sabadini, E., Hubinger, M.D., Cunha, R.L., in press. Stress relaxation of acid-induced milk gels. *Food and Bioprocess Technology*, doi:10.1007/s11947-010-0342-4.

Şen, M., Erboz, E.N., 2010. Determination of critical gelation conditions of κ-carrageenan by viscosimetric and FT–IR analyses. Food Research International 43 (5), 1361–1364.

Smrdel, P., Bogataj, M., Zega, A., Planinsek, O., Mrhar, A., 2008. Shape optimization and characterization of polysaccharide beads prepared by ionotropic gelation. Journal of Microencapsulation 25 (2), 90–105.

Steffe, J.F., 1996. Rheological Methods in Food Process Engineering. Freeman Press, East Lansing.

Varga, C.M., Lasheras, J.C., Hopfinger, E.J., 2003. Initial breakup of a small-diameter liquid jet by a high-speed gas stream. Journal of Fluid Mechanics 497, 405–434.

Wolf, B., Frith, W.J., Singleton, S., Tassieri, M., Norton, I.T., 2001. Shear behavior of biopolymer suspensions with spheroidal and cylindrical particles. Rheologica Acta 40 (3), 238–247.

Zhang, J., Li, X., Zhang, D., Xiu, Z., 2007. Theoretical and experimental investigations on the size of alginate microspheres prepared by dropping and spraying. Journal of Microencapsulation 24 (4), 303–322.